

FINAL REPORT

Effects of Global Change on Extreme Precipitation and Flooding:
New Approaches to IDF and Regional Flood Frequency
Estimation

SERDP Project RC-2513

SEPTEMBER 2020

Dennis Lettenmaier
University of California, Los Angeles

Distribution Statement A

This document has been cleared for public release



This report was prepared under contract to the Department of Defense Strategic Environmental Research and Development Program (SERDP). The publication of this report does not indicate endorsement by the Department of Defense, nor should the contents be construed as reflecting the official policy or position of the Department of Defense. Reference herein to any specific commercial product, process, or service by trade name, trademark, manufacturer, or otherwise, does not necessarily constitute or imply its endorsement, recommendation, or favoring by the Department of Defense.

REPORT DOCUMENTATION PAGE

*Form Approved
OMB No. 0704-0188*

The public reporting burden for this collection of information is estimated to average 1 hour per response, including the time for reviewing instructions, searching existing data sources, gathering and maintaining the data needed, and completing and reviewing the collection of information. Send comments regarding this burden estimate or any other aspect of this collection of information, including suggestions for reducing the burden, to Department of Defense, Washington Headquarters Services, Directorate for Information Operations and Reports (0704-0188), 1215 Jefferson Davis Highway, Suite 1204, Arlington, VA 22202-4302. Respondents should be aware that notwithstanding any other provision of law, no person shall be subject to any penalty for failing to comply with a collection of information if it does not display a currently valid OMB control number.
PLEASE DO NOT RETURN YOUR FORM TO THE ABOVE ADDRESS.

1. REPORT DATE (DD-MM-YYYY) 21-Sep-2020		2. REPORT TYPE SERDP Final Report		3. DATES COVERED (From - To) 8/31/2015 - 8/31/2020	
4. TITLE AND SUBTITLE Effects of Global Change on Extreme Precipitation and Flooding: New Approaches to IDF and Regional Flood Frequency Estimation				5a. CONTRACT NUMBER 15-C-0053	
				5b. GRANT NUMBER	
				5c. PROGRAM ELEMENT NUMBER	
6. AUTHOR(S) Dennis Lettenmaier				5d. PROJECT NUMBER RC-2513	
				5e. TASK NUMBER	
				5f. WORK UNIT NUMBER	
7. PERFORMING ORGANIZATION NAME(S) AND ADDRESS(ES) University of California, Los Angeles Department of Geography 1255 Bunche Hall, Box 951524 Los Angeles, CA 90095-1524				8. PERFORMING ORGANIZATION REPORT NUMBER RC-2513	
9. SPONSORING/MONITORING AGENCY NAME(S) AND ADDRESS(ES) Strategic Environmental Research and Development Program (SERDP) 4800 Mark Center Drive, Suite 16F16 Alexandria, VA 22350-3605				10. SPONSOR/MONITOR'S ACRONYM(S) SERDP	
				11. SPONSOR/MONITOR'S REPORT NUMBER(S) RC-2513	
12. DISTRIBUTION/AVAILABILITY STATEMENT DISTRIBUTION STATEMENT A. Approved for public release: distribution unlimited.					
13. SUPPLEMENTARY NOTES					
14. ABSTRACT The civil infrastructure of our country is by large built by stationary standards to address weather and climate related risks. However, with increasing effects of climate change being manifested, we are interested in re-assessing the risk of projects that are based on stationary intensity-duration-frequency curves to manage events such as extreme precipitation and flooding via runoff. Our objectives are to (1) develop protocols for incorporating nonstationarity into extreme value theory, which can be applied to flood frequency as well as extreme precipitation events; and incorporate ongoing and future projections of climate warming on flood frequency estimates for watersheds affected by (2) rain-on-snow events and (3) atmospheric rivers.					
15. SUBJECT TERMS Annual Maximum Series, Atmospheric River, Cascade Range, Civil Engineering, Climate Change, Design Storm, Global Warming, Elevation Band, Extreme Precipitation, Extreme Value Theory, Flood Risk Design, Frequency Analysis, Historical Station Observations, Hydrological Modeling, IDF Curves, Integrated Water Vapor Transport, Monte Carlo Simulations Nonstationary Design, Pacific Northwest, Rain-on-Snow, Regional Climate Model Downscaling, Runoff Events, Sierra Nevada Range, Significant Influence Zone, Snowpack Accumulation, Snowmelt, Snow Water Equivalent, Trends in Extreme Precipitation					
16. SECURITY CLASSIFICATION OF:			17. LIMITATION OF ABSTRACT UNCLASS	18. NUMBER OF PAGES 38	19a. NAME OF RESPONSIBLE PERSON Dennis Lettenmaier
a. REPORT UNCLASS	b. ABSTRACT UNCLASS	c. THIS PAGE UNCLASS			19b. TELEPHONE NUMBER (Include area code) 310-825-1071

Table of Contents

Table of Contents	ii
List of Figures	iii
List of Acronyms	iv
Keywords	vi
Acknowledgments	vi
Abstract	vii
Executive Summary	viii
Final Report	
Introduction/Objectives	1
Background	1
Materials and Methods	2
Results and Discussion	3
Chapter 1 – Extreme Precipitation Events	4
Chapter 2 – MET STATS	9
Chapter 3 – Atmospheric River Events	9
Chapter 4 – Rain-on-Snow Events	12
Conclusions/Implications	16
Literature Cited	19
Appendices	
Supporting Data	
List of Publications	
Other Supporting Materials	

List of Figures

Figure 1: the ratio of how much larger the nRMSE is in misapplying the NS-GEV versus correctly applying the S-GEV distribution for the 10-year storm (top) and 100-year storm (bottom).	5
Figure 2: the absolute values of nRMSE from applying an NS-GEV model to an S-GEV environment for the 10-year storm (top) and 100-year storm (bottom) as a function of record length	6
Figure 3: absolute values of nRMSE for the 10-year storm as a function of record length under the three nonstationary scenarios with NSI = 0.1. Scenario I (top), II (middle) and III (bottom) are all shown under these described conditions.	7-8
Figure 4: reproduced from Eldardiry et al., 2019. Fraction of AR dates from all dates producing the upper 10 th percentile of daily precipitation for each latitudinal band by cold season month	10
Figure 5: reproduced from Eldardiry et al., 2019. Average of upper 10th percentile positive and negative changes in daily SWE during the upper 10th percentile of daily precipitation on AR dates by winter month.	11
Figure 6: reproduced from Eldardiry et al., 2019. (left) The 1-day AR precipitation depths and frequencies by AR landfalling latitude (return periods are indicated by different colors). (right) As in the left panel, but for 3-day totals.	11
Figure 7: reproduced from Eldardiry et al., 2019. Daily precipitation associated with AR dates during dry and wet years in three mountainous subregions (North Cascades, South Cascades, and Sierra Nevada). On each box, the central mark indicates the median depth, and the bottom and top edges of the box indicate the 25th and 75th percentiles (or interquartile range), respectively.	12
Figure 8: reproduced from Li et al., 2019. Fractional contribution of the number of large and extreme ROS days to the number of (a) total large runoff days, (b) total extreme runoff days, (c) total large runoff, (d) total extreme runoff. The white areas in the maps have mean annual maximum snow water equivalent less than 20 mm and are excluded in the analysis.	14
Figure 9: reproduced from Li et al., 2019. Fractional contribution to the large and extreme ROS runoff from rainfall and snowmelt. (a) and (b) show the ratio of the rainfall and snowmelt from the large ROS to the total large ROS respectively. (c) and (d) show the ratio of the rainfall and snowmelt from the extreme ROS days (i.e., the ROS days in the 20 extreme runoff days) to the total extreme ROS runoff (i.e., the total runoff from the extreme ROS days), respectively. White areas in the maps have mean annual maximum snow water equivalent less than 20mm and are excluded from the analysis.	15
Figure 10: reproduced from Li et al., 2019. Change in the ratio of total runoff during large ROS days (left) and extreme ROS days (right) to total runoff from the 200 large (or extreme) runoff days. White areas have historical mean annual maximum snow water equivalent less than 20 mm and are excluded in the analysis	16

List of Acronyms

AMS	Annual Maximum Series
AR	Atmospheric River
ARF	Areal Reduction Factor
CC	Clausius-Clapeyron
CEC	Commission for Environmental Cooperation
CESM	Community Earth System Model
CLASS	Canadian Land Surface Scheme
CM	Climate Model
CMIP5	Coupled Model Intercomparison Project phase 5
CONUS	Continental United States
COOP	Cooperative Observer
CV	Coefficient of Variation
DOD	Department of Defense
DHSVM	Distributed Hydrology Soil Vegetation Model
EPA	Environmental Protection Agency
EVT	Extreme Value Theory
GAGES	Geospatial Attributes of Gages for Evaluating Streamflow Version II
GCM	Global Climate Model
GEV	Generalized Extreme Value
GUM	Gumbel
HCN	Historical Climatology Network
IDF	Intensity-Duration-Frequency
IDAF	Intensity-Duration-Area-Frequency
IVT	Integrated Water Vapor Transport
IWV	Integrated Water Vapor
LGN	Lognormal
LGS	Logistic
MC	Monte Carlo
MET-STATS	
MK	Mann-Kendall
NCAR	National Center for Atmospheric Research
NCEP	National Center for Environmental Prediction
NEVA	Nonstationary Extreme Value Analysis
NS	Nonstationary
NOAA	National Oceanic and Atmospheric Administration
NOAH-MP	Noah Multiparameterization
NRMSE	Normalized Root Mean Square Error
PEA	Pearson III
PRISM	Parameter-elevation Regressions on Independent Slopes Model
PNW	Pacific Northwest
RCM	Regional Climate Model
ROS	Rain-on-Snow
S	Stationary

SWE	Snow Water Equivalent
SNSR	Sierra Nevada SWE Reanalysis
US	United States
USGS	United States Geological Survey
VIC	Variable Infiltration Capacity
WRF	Weather Research and Forecasting

Keywords

Annual Maximum Series, Atmospheric River, Cascade Range, Civil Engineering, Climate Change, Design Storm, Global Warming, Elevation Band, Extreme Precipitation, Extreme Value Theory, Flood Risk Design, Frequency Analysis, Historical Station Observations, Hydrological Modeling, IDF Curves, Integrated Water Vapor Transport, Monte Carlo Simulations, Nonstationary Design, Pacific Northwest, Rain-on-Snow, Regional Climate Model Downscaling, Runoff Events, Sierra Nevada Range, Significant Influence Zone, Snowpack Accumulation, Snowmelt, Snow Water Equivalent, Trends in Extreme Precipitation, Western US,

Acknowledgements

This research was supported by the Strategic Environmental Research and Development Program (SERDP)–Project #RC-2513 granted to the University of California, Los Angeles, and an associated subcontract to the University of Washington. Support also came from the NASA Grant NNX16AC63G to the University of Washington and from the U.S.-China Clean Energy Research Center for Water-Energy Technologies/California Energy Commission Grant 300-15-006. The authors declare no real or perceived financial conflicts of interests.

Abstract

Introduction and Objectives

The civil infrastructure of our country is by large built by stationary standards to address weather and climate related risks. However, with increasing effects of climate change being manifested, we are interested in re-assessing the risk of projects that are based on stationary intensity-duration-frequency curves to manage events such as extreme precipitation and flooding via runoff. Our objectives are to (1) develop protocols for incorporating nonstationarity into extreme value theory, which can be applied to flood frequency as well as extreme precipitation events; and incorporate ongoing and future projections of climate warming on flood frequency estimates for watersheds affected by (2) rain-on-snow events and (3) atmospheric rivers.

Technical Approach

Our technical approach includes two main elements to address our first objective and a third element to address the second objective. The first element incorporates nonstationarity as observed in historical records of extreme precipitation into the protocols for intensity-duration-frequency relationships via the examination of the underlying probability distribution function. The second element involves the incorporation of regional climate models into flood risks; we analyze the effects of atmospheric rivers on flooding/extreme precipitation in the western United States. The third element is specific to flood frequency estimation in watersheds affected by rain-on-snow events and snowmelt. We employ a hydrological model to track both the contributions of rain-on-snow events and snowmelt to runoff and assess the sensitivity of this relationship to increases in temperature.

Results

We divide our results into three main sections, each of which address different aspects of flood risk with climate change via different hydrological processes: extreme precipitation, atmospheric rivers, rain-on-snow events. We find the tradeoff in the increasing variability versus decreasing bias from including a time-varying parameter in extreme precipitation distributions for both stationary and nonstationary environments. We conduct a study on the patterns of behavior of landfalling atmospheric rivers along three sections of mountains in the west coast. We separate the contribution of snowmelt versus rain-on-snow events on flooding events across the United States and discuss the differences.

Benefits

Our work incorporates time-dependent relationships into the best current extreme precipitation and flood frequency estimation methods. The results of this work benefit risk-based flood design not only at Department Of Defense and other governmental facilities, which will surely be impacted by changing flood risk in the face of climate warming, but also across the field of hydrologic engineering design.

Executive Summary

Introduction

Floods are a costly natural hazard, having caused more than a billion dollars of damage in the United States since the 1980s. There are multiple causes behind flooding events, so while the literature on the changing magnitudes of flooding events has remained mixed (e.g. Lins and Slack, 1999; 2005; Hirsch and Ryberg, 2012), we have found specific mechanisms such as extreme precipitation storms, landfalling atmospheric rivers (ARs), and rain-on-snow (ROS) events are changing in magnitude due to changes of temperature with time (e.g. Kunkel et al., 1999; Mishra and Lettenmaier, 2011; Westra et al., 2013; Groisman et al., 2014). Engineering standards to address flooding from these events as well as others are designed to address risk assessments that are built with stationary assumptions. However, increasing evidence points to nonstationary relationships occurring due to increasing temperature with time, i.e. climate change. Increased temperatures lead to increases in saturated water vapor following the Clausius-Clapeyron relationship at around a 7% increase in saturated water vapor per degree Celsius increase (Trenberth, et al., 2003).

The changes in saturated water vapor can lead to increases in extreme precipitation events and has been studied both in historical observations, gridded datasets, and model predictions. Studies have found that increases have been observed in extreme precipitation, either in intensity or frequency, or both (e.g. Karl and Knight, 1998; Easterling et al., 2000; Frich et al., 2002; Min et al., 2011; Easterling, et al., 2017). ARs are also impacted by changes in temperature due to the Clausius-Clapeyron relationship. When an AR event makes landfall, the transportation of large amounts of water vapor can lead to heavy precipitation and flooding. Several studies highlight the importance of landfalling AR events and intense precipitation or flooding events in the western US (Ralph et al. 2006; Neiman et al. 2008, 2011; Barth et al. 2017; Konrad and Dettinger 2017; Lamjiri et al. 2017). ROS events can include intense rainfall and rapid snowmelt that contributes to flooding that further lead to increased risk for landslides, river channel morphology changes, and increased risk of avalanche triggers (Harr, 1981; Bergman, 1987; Conwat et al., 1988; Conway and Raymond, 1993; Heywood, 1988; Singh et al., 1997). There is now a need to update risk assessment protocols so that they will be appropriate for the designing and planning of civil infrastructure over the project's planned lifespan.

Objectives

Our overall objectives are to (1) develop protocols for incorporating nonstationarity into extreme value theory, which can be applied to flood frequency as well as extreme precipitation events; and incorporate ongoing and future projections of climate warming on flood frequency estimates for watersheds affected by (2) rain-on-snow events and (3) atmospheric rivers. These objectives are created as a means of responding to the scientific questions related to how can engineering design criteria associated with extreme precipitation and flooding be adjusted to reflect observed and projected effects of climate change in a manner that is consistent with standards of engineering practice? We employ statistical methods, Monte Carlo simulations, at-site and regional trend analysis, use of regional climate models, downscaling technology, delta-warming method, and the VIC hydrological model to meet our three objectives. For our work, we merge historical station data, reconstructed historical data, gridded observation data, and model projections to create a long time series that is consistent throughout past to future time periods.

Technical Approach

We break our technical approach down into three main elements. In the first element, we incorporate nonstationarity into extreme value theory by introducing a time-varying parameter into the generalized extreme value distribution family. We use this modified distribution to model extreme precipitation events, AMS in particular, as pulled from historical observations. In particular, we assess the model performance differences in applying a nonstationary model to a stationary environment and vice versa, explicitly finding which has a larger penalty as quantified in nRMSE of the 10-year and 100-year design storms. This element addresses extreme precipitation events and is meant to be applied to short-term IDF curve-based risk assessment.

In the second element, we must first define how we categorize an event as an AR based on thresholding IVT as well as spatial features. Then for each AR landfalling date, we pull from relevant hydrometeorological variables such as precipitation through the dynamic downscaling (via WRF) of the NCEP-NCAR atmospheric reanalysis. The WRF parameterization is based on a previous study and produces simulated results that are near observations. We then characterize daily aggregated changes in precipitation and SWE for each AR event over our domain. We assess the severity of AR-induced precipitation by looking at other flood events that did not occur during a landfalling AR. We further look to assess the different impacts that ARs have on precipitation intensity via characteristics such as latitude, elevation, and dry or wet conditions.

The third element addresses the risk of ROS to flood frequency estimation in affected watersheds. We characterize ROS events as having a minimum amount of rainfall on a minimum depth of a snowpack for which snowmelt makes up at least 20% of the total rainfall and snowmelt of the day. We use the VIC hydrological model to simulate SWE and runoff variables across the CONUS with relevant variables related to snow mass and energy balance processes being tracked throughout the time period of the simulation. We compare the SWE and runoff to historical observations as well as the SNSR reanalysis dataset to check the quality of modeling and parameterization used. Similar to the first task, we use the updated NS-GEV distribution to model flood risk changes with time. We apply a delta-warming method in which the air temperature is increased while other variables are left the same to assess how sensitive ROS are to impending global warming.

Results and Discussion

The main takeaway conclusions from the first element are concerning the misapplication of either the S-GEV or NS-GEV distribution with regards to environments with different, realistic values of CV, skewness, record length, and time. The application of S-GEV is associated with lower variance but larger bias in the resulting error. The application of NS-GEV is associated with increased variance, due to the inclusion of a fourth parameter, but possibly lower bias in error. Error in this element is defined as the nRMSE of the estimations of the 10-year and 100-year design storm. We found that for short record lengths of thirty years, while the NS-GEV is capable of modeling near-stationary conditions, the increased variance is too high to offset any decrease in bias. For a record length of fifty years, the tradeoff between variance and bias is closer to being equal and the question of which application is safer if the underlying distribution is unknown depends on many other factors such as the CV, skewness, and amount of nonstationarity present. For the longest record length option used of 100 years, the nRMSE of the 10-year and 100-year design storm is much larger at the initial time ($t = 0$ indicating the beginning of the record length) for the misapplication of the S-GEV than that of the NS-GEV. As time increases, the ranges of nRMSE stabilize to be around 0.1 regardless of the data

characteristics. For large amounts of nonstationarity, the application of NS-GEV is preferred over S-GEV regardless of other characteristics of the environment.

Overall, in deciding which model of the GEV distribution to apply to an AMS with unknown underlying distribution, the decision should take into particular consideration the record length available as well as the project lifespan required. To a smaller degree, they will benefit from knowing the data CV and skewness. For scenarios most representative of current conditions, the S-GEV should be applied if the record length is under 50 years for more accurate design storm estimates. When the record length is at least 50 years, the additional complications of the relationship between nRMSE and CV, skewness, and time must be considered carefully before deciding which GEV model to use. The application of the NS-GEV can be used when the record length is long enough to reduce the additional variance inherent in the model; we found that a record length of 100 years would be sufficient. Further, as the degree of nonstationarity, quantified as the NSI, increases or the lifespan of the project increases, the NS-GEV tends to lead to more accurate design storms. For environments where the data is not truly GEV-based, stationary or nonstationary, we found that the S-GEV is fairly robust and capable of estimating design storms with similar accuracy for NS-GUM, NS-LGN, and NS-LGS data. For larger storms, there should be increased caution if the environment is NS-LGN. For environments where the behavior of the data is truly NS-PEA, however, the application of a GEV distribution is inappropriate.

In our work downscaling NCEP-NCAR reanalysis data using the WRF model, we focused on the time period of 1949 to 2015 and over three subregions in coastal western US: northern Cascades, southern Cascades, and the Sierra Nevada mountains. We found that landfalling ARs in the Sierra Nevada subregion had higher precipitation amounts than in the Cascade ranges, despite more AR events occurring in the Cascades. At latitudes below 42.5 degrees N, the most extreme events take place in January and February. The largest increase in SWE related to AR events occurs in January, and again the Sierra Nevada subregion sees the largest increase in SWE out of the three subregions. Decreases in SWE are also capable of occurring due to ARs during the cold months and can lead to extreme snowmelt conditions that is related to early snowmelt and increased chances of ROS conditions.

We found that ARs are a key component of water resource management in the western US due to their ability to increase early snowmelt, increase flood risk, and to end droughts. We categorize ARs by wet versus dry years and find that in the Sierra Nevada subregion, ARs during wet years occur more frequently than in dry years and also produce heavier precipitation and snow accumulation per landfalling event. In contrast, in the Cascade subregions, precipitation amounts are fairly comparable between wet and dry years. In the Cascades, the number of AR events are also smaller for dry years than wet years. Our final concluding observation on the differences between AR characteristics amongst the subregions is that most AR extreme precipitation events in the northern subregions are produced during warm AR dates as compared to all upper 10th percentile precipitation. Warm AR events result in lower SWE accumulation and higher snowmelt rates particularly for northern latitudes over both Cascade subregions.

In our research into ROS events, we find that VIC hydrological model was quite capable of providing believable details of snow mass and energy transfer and produced results that were similar to the SNSR SWE data in both spatial and temporal patterns. The total SWE between VIC results and SNSR data are consistent over the common overlapping period. Further, the timing of the annual max SWE of the VIC results correlate highly with the timing of SNSR max SWE, being mostly within two days (earlier or later) than each other.

Typically, due to the elevation profiles of the mountain ranges, the western mountains have largest snow accumulations and are most impacted by ROS events with mid-elevation transition zones having the largest ROS flood-generating potential. ROS in the mountains of the West occur most often in early spring – as opposed to in fall and winter for the coastal West and general Eastern US. Outside of the western mountains, there are mountain ranges in the Northeast, upper Midwest, and Appalachian region that are affected by ROS events. Altogether, these regions stand to be most impacted by future changes in ROS characterizations. We identify in particular a “significant influence zone” as being western US mountain ranges with elevations between 1,000 and 1,500 meters. With global warming, it is likely that this zone will shift upwards to be above 2,000 meters in the future as snowpack depths decrease at lower elevations.

We found from our historical period that over half of what we defined as “large” runoff days (upper 1 percentile) and over three-quarters of “extreme” runoff days (upper 0.1 percentile) are related to ROS events within our study area of the above-mentioned mountain regions. However, the total runoff from ROS days only accounts for less than a quarter of the runoff from large runoff days and barely five percent of the runoff for extreme runoff days. This implies that most extreme runoff is a result of intense rainfall or radiation-driven snowmelt even on ROS days. In the west coast, the extreme runoff generated during ROS days is mostly due to extreme rainfall, while along the east coast, extreme runoff is associated with snowmelt. The snowmelt in the east coast is dominated by both net radiation and turbulent heat flux, as opposed to the snowmelt in the west coast which is dominated only by net radiation. We found that the amount of snow directly melted by rainfall through heat advection is negligible.

With global warming, ROS events will play an increasingly large role in high-elevation mountains (over 2,000 m) and decreasing roles for low to moderate elevations below 2,000 m. It is likely that the effects of ROS, due to this conditioning on elevation bands, will decrease across most of the Midwest and eastern US. However, in the western US, the runoff contribution from ROS to extreme flooding events will increase. Further, the timing of the ROS will shift earlier by about a month when under our specified delta-warming methods where temperatures are uniformly increased by 2 degrees Celsius across the CONUS.

Implication for Future Research and Benefits

Our work across all facets has implications for water management and civil engineering design standards. Establishing a nonstationary probability and cumulative distribution function has direct implications for the construction of IDF and IDAF curves, which are essential to the sizing of any engineering project dependent on precipitation intake. The application of the NS-GEV distribution to AMS will help practitioners in the public and private sector understand how flood risk related to extreme precipitation will change with time by being a tool with which to model how design storms are estimated to change with time. Without this updated methodology, projects in areas of increasing flood risk will be under-prepared for design storms while projects in areas of decreasing extreme precipitation intensity will be over-prepared and likely more costly than necessary. This work is a vital component of understanding how risk assessment will change in the short-term future as we aim to provide guidance of when there will be a larger penalty for staying with a S-GEV model versus implementing an NS-GEV model. Further research in this area could include more assessments of how a five-parameter NS-GEV model, with a time-varying index in both the location and scale parameter, performs compared to the four-parameter NS-GEV and the three-parameter S-GEV. Research could also be conducted in what the penalties are when using nonstationary versions of other commonly used distributions

for modeling extreme precipitation such as the NS-GUM, NS-LGN, and NS-LGS. Further work should be done to apply the methods discussed to regional precipitation.

Given the associated extreme precipitations with ARs, a better understanding of ARs will be essential to water management in the western US. Our research in this area has further implications in flood and drought risk assessment due to the ARs role as a drought-buster in the west, and in operational weather forecasting. Water resource management needs to include the effects of ARs for higher accuracy. Key to this is first the ability to detect and forecast ARs and second the understanding of the relationship between precipitation and ARs based on local conditions such as elevation, latitude, and other conditions such as being a warm versus dry year. In particular, to improve water resource management, one will need to incorporate our work here and that of future research in order to have better forecasting and management of AR induced precipitation, snow melting rate, and shifting of timing of peak SWE – all three are elements that play an important role in the water resources of the western US. It is likely that with climate change leading to increasing temperatures, landfalling AR events will lead to increased induced precipitation and to higher elevations being needed for orographic precipitation. Snow melting rates will likely increase, shifting important snowpack characteristics including timing of peak SWE, and will impact the profile of any snow-melt related runoff. The melting snowpack lead to spring runoff that is vital in understanding and managing water resources in the west. Future work should be done for a more detailed understanding of the impacts of AR precipitation and runoff on modeling the water budget in the western US. Further, these hydrological changes will affect reservoir operations. Highlighting the spatial differences in AR characteristics will be key in developing better forecasting methods of AR-related changes, and further research is needed to provide this information.

ROS events impact the major western mountain ranges of the US as well as some mountain ranges in the upper Midwest and along eastern US. Our research on ROS has implications for water resource management in these regions, especially at elevations of 1,000 to 1,500 m presently (shifted up to 2,000 m in warmer climates). Understanding the influence of ROS on runoff plays a modest role in large runoff events and a small role in extreme runoff days. In a warmer future, the role of ROS in runoff will become increasingly important at high elevations and along the west coast. Further the change in the timing of ROS shifting to be earlier will impact the characteristics of snowpack accumulation and depletion which has implications on water resource management particularly in the west. Future work done based on how ROS will respond to global warming as predicted by GCMs or RCMs will be a valuable extension of the sensitivity analysis we conducted using the delta warming method.

Final Report

Introduction/Objective

Floods are an extremely costly natural hazard and can be life-threatening. There are some clear patterns of changes in flooding across the western US under projected climate change (Hamlet and Lettenmaier, 2007), but overall, there is a lack of literature on the possible changes of flood risk with increasing temperatures. Our overall objectives remain very similar to our original objectives, but over the course of the project we may have changed them in light of results found. Thus we aimed to (1) develop protocols for incorporating nonstationarity into extreme value theory, which can be applied to flood frequency as well as extreme precipitation events; and incorporate ongoing and future projections of climate warming on flood frequency estimates for watersheds affected by (2) rain-on-snow events and (3) atmospheric rivers.

The original proposal broke down our work into nine tasks, including Task 1 as being the acceptance of subcontracts. As we progressed in our research, we found that it was more natural to regroup these task items as based on topic rather than as sequential steps. To that end, we will structure our report into four main chapters, which together do cover the original task items. In the first chapter, we discuss the nonstationary behavior that can be found in extreme precipitation events through both historical station data and using regional climate model-based projections. Chapter 1 covers Task 2 (Site selection), Task 3 (Develop and test a time-varying GEV-based regional frequency approach), and Task 4 (Evaluate scaling relationships for implementation of IDF and IDAF analysis). Chapter 2 - MET STATS. Chapter 3 is centered on how climate change and atmospheric rivers have affected precipitation and flood frequencies via analysis of both station data and simulated historical data over the same range. This chapter effectively covers Task 5 (Evaluate the consistency of methods developed in Tasks 3 and 4 for use with RCM output), Task 6 (Develop a seamless approach to merging regional IDF and IDAF relationships), and Task 7 (Evaluate uncertainty in IDF and IDAF estimates over the WRF domain). In our final chapter on how climate change affects rain-on-snow events and thereafter floor frequencies, we cover the remaining Task 8 (Adapt Hamlet & Lettenmaier (2007) approach to evaluate changes in snowmelt-related flood risk over the CONUS) and Task 9 (Evaluate snowmelt-affected flood frequency changes over the CONUS).

Background

Because of climate change, there is a need to assess what trends can be established or are projected for various hydrological variables in the interest of accurate water resource management. With increasing temperatures, there is an associated increase in saturated water vapor pressure that roughly follows the Clausius-Clapeyron (CC) relationship at about a 7% increase in saturated water vapor per degree of Celsius increase (Trenberth et al., 2003). Studies are emerging in establishing a trend between certain hydrological events like flood events or extreme precipitation events and an index that is often either time or temperature. Modeling with temperature typically leads to lower uncertainties in projections as temperature and saturated water vapor pressure have a well-known and established relationship. Min et al. (2011) show that global warming is linked to the intensification of intense extreme precipitation events across much of the Northern Hemisphere. Kunkel (2003) established increases in the frequency of extreme precipitation events since the 1920s in the CONUS. Armstrong et al. (2014) found that in the northeastern US, the annual flood magnitude had increasing trends at 75% of the gages tested. Further, they link hydroclimatic changes in flooding to changes in both cyclic

atmospheric variability and to anthropogenic climate change which affect antecedent conditions and event-scale processes.

Materials and Methods

The materials used over the course of this research project include multiple datasets that cover historical observations as well as climate model projections. We used both point data, areal data, and a distinct type of gridded data. One of the at-site observation-based data we used consists of a set of quality-checked hourly precipitation data established by Mishra et al. (2012) which has stations distributed across CONUS. The quality checks imposed are regarding flagged data and completeness of record. The stations are all managed by NOAA and include stations within subsets of NOAA data such as being in the COOP network or the HCN network. Station density is uniform across the CONUS but with sparser coverage in the mountainous regions of the western US. The stations span a 60-year period from 1950 to 2009, although no station has complete coverage over these 60 years. We extended the dataset through 2013 using the NOAA dataset available via File Transfer Protocol (meaning available in bulk). We used a gridded data set as created by Livneh et al. (2015), that has fields of temperature and precipitation at a 1/16th degree spatial resolution and daily time resolution. From this data set, we used grid cells that cover CONUS entirely. The Livneh et al. (2015) data uses the PRISM methodology established in Daly et al. (1997) and observation-based climatology values. We also made use of the Livneh et al. 2013 dataset specifically for their SWE variable which is model-generated. Another data set we used for SWE comparisons is the Sierra Nevada SWE reanalysis (SNSR) established in Margulis et al., 2016, which is based on Landsat satellite observations. It covers portions of the Sierra Nevada range with a high spatial resolution of 90 meters and is available for the period of 1985 to 2015.

In delineating the Cascades and Sierra Nevada subregions, we used the boundaries from the Commission for Environmental Cooperation Ecological Regions of North America, Level III (McMahon et al., 2001; Omernik, 2004). For streamflow observations, we used the Geospatial Attributes of Gages for Evaluating Streamflow Version II (GAGES II; Falcone et al. (2010)) data set which is made by the USGS and has over 9,000 streamflow gages across the CONUS. From this network, we selected 311 gages that serves as reference gages, have no or minimal upstream regulation or diversions, and with over 50 years of data over the time period of 1950 to 2009. To determine AR events, we used the IVT-based AR catalog established in Guan and Waliser (2015) as well as the IWV-based Neimen et al. (2008) catalogue. Guan and Waliser (2015) ARs are identified based on imposing thresholds at the 85-percentile specific to both season and location with a fixed lower bound. The Neimen et al. (2008) catalogue has a minimum threshold of IWV being over 2 cm. They also used physical characteristics to find ARs by specifying that the ARs be over 2000 km long and under 1000 km wide. This catalogue was extended in Dettinger et al. (2011), and we used this extension as well. Further, we used the NCEP-NCAR reanalysis covering the water years of 1949 to 2015 which gives us necessary hydrometeorological variables needed for our modeling work. This data set has a temporal resolution of 6-hour timesteps and a spatial resolution of 2.5 latitude-longitude degrees.

Extreme precipitation analyses made use of extreme value theory (EVT) and we specifically employed the Generalized Extreme Value (GEV) distribution for assessing risk. The parameters of the GEV distribution can be estimated from observational data via L-moment analysis (Hosking and Wallis, 1997). The NS-GEV distribution has an additional time-varying fourth parameter that can be estimated in a Matlab software package called NEVA, described in

Cheng et al., 2014. NEVA uses a Bayesian approach with a differential evolution Markov Chain (Ter Braak, 2006; Vrugt et al., 2009). For trend analysis, we applied the Mann-Kendall trend test across AMS at various significance levels but mainly at alpha of 0.05 or 0.10. For the work involving Monte Carlo simulations, we computed the mean, variance, and skewness of the AMS extracted from observational data in order to create realistic environments. We considered 300 unique combinations of mean, CV, and skewness. Using the relationships of these statistical characteristics with relevant probability distribution functions, we were able to solve for the matching parameters of the GEV, GUM, LGN, LGS, and PEA distributions. For each unique parent distribution, we generated 10,000 synthetic observation sequences of either 30, 50, or 100 observations for three distinct scenarios involving nonstationarity within the mean and/or the CV and standard deviation. We then fit the S-GEV or NS-GEV as appropriate to the synthetic data and discuss the errors in the 10-year and 100-year design storms.

We used the WRF model for dynamic downscaling using the NCEP-NCAR data as initial and boundary conditions. In some exploratory work, we found that using nested domains, originally proposed as an option, gave little to no benefits over using a single domain. We continued with WRF simulations over a single domain over the western US at a resolution of 15 km. We selected the Morrison double-moment scheme (Morrison et al., 2009) option 10 for microphysics and the Kain-Fritsch (Kain and Fritsch 1990, 1993) option 1 for cumulus physics. For the planetary boundary layer, we chose the Yonsei University (Hong et al., 2006) scheme. We used Noah-MP v 1.6 land surface model with the Monin-Obukhov option 1 for surface layer drag, the CLASS option for ground surface albedo, and the Jordan model (Jordan, 1991) option 1 for precipitation partitioning between snow and rain. We ran simulations over 1949 to 2015 and produced hourly output variables for the water season of October 15 to April 1. The first 15 days of outputs are used as model spinup and discarded. We aggregated the hourly precipitation and SWE outputs from WRF and conduct our statistical analyses based mainly on these two variables. Other variables we evaluated are AR storm duration and frequency, and surface air temperature.

We used the VIC hydrological model (Liang et al., 1994; Andreadis et al., 2009), v 4.2d, to simulate SWE and runoff across the entire CONUS. Specifically, we used the VIC snow model with detailed snow mass and energy balance processes which account for mass and energy transfers to and from the atmosphere as well as the intervening effects of overlying vegetation. Each VIC grid cell has five elevation bands and 12 vegetation tiles to characterize the terrain and vegetation on a sub-pixel level. We allowed for partial snow coverage function for more realistic snow spatial variability in our simulations. The VIC model as we implemented it required four forcing variables – maximum and minimum temperature, precipitation, and wind speed. We supplemented other variables from calculations from the mountain microclimate simulation model (Hungerford et al., 1989). For simplification, we did not route through stream networks but rather model output streamflow using the direct aggregation of runoff and baseflow over the drainage area over relevant gages. From the output of the VIC modeling, we used SWE and precipitation to find ROS events with flood-generating potential. We characterized some aspects of ROS behavior in the western US by finding the frequency of days per year and the centroid of the timing. We analyzed various aspects of the upper percentiles of runoff generated by both ROS and total (non-ROS) days. We calculated the contribution of both rainfall and snowmelt to these extreme runoff events.

Results and Discussion

Chapter 1 - Extreme Precipitation Events

We make use of EVT based on AMS as constructed from a historical record of rain gauges across the CONUS and both introduce and discuss the implications of adding the ability to be nonstationary. Specifically, we focus on GEV type II distribution, hereafter just labeled GEV, which has three parameters: location, scale, and shape. We introduce a time-dependent variable into the location parameter thus increasing the number of parameters for a NS-GEV to be four. There are many methods to determine which distribution may be the best fit for extreme rainfall data, but the truth is that the underlying distribution is always unknown. The application of S-GEV and the NS-GEV have their own advantages and disadvantages. The S-GEV, due to its smaller number of parameters, has more steady amounts of variance over-estimates. However, due to its inability to capture nonstationary behavior, use of the S-GEV in a NS-GEV environment will have increasingly large biases as time continues. On the other hand, the NS-GEV, due to the inclusion of a fourth parameter, has inherently higher variance across estimates, but is better able to capture either stationary or nonstationary behavior and thus have lower bias. We answer the question: which misapplication leads to larger errors?

We used Monte Carlo simulations to set up different scenarios of S- and NS- rainfall, fit NS-GEV or S-GEV distributions to the data and find the estimated 10-year and 100-year storm. We evaluated the performance of the models by the normalized root mean square (nRMSE) of these two storms. The scenarios we consider are (1) S-GEV environment with NS-GEV modeling, and (2) S-GEV modeling for an NS-GEV environment where (a) only the mean is increasing, (b) the mean and std are increasing, and (c) the mean, std, and CV are increasing. The penalty ratio of misapplication for the stationary scenario is shown in Figure 1 and the nRMSE values are shown in Figure 2. The parameter space, mean, CV, and skewness, we defined for the simulations were based on the range of the parameters we found from 1000+ stations across the CONUS. We used three record lengths in our simulations of 30, 50, and 100 years. We show the resulting nRMSE patterns of the 10-year design storm for all these nonstationary scenarios in Figure 3. We found that at a record length of 30 years, the variance is too high to warrant applying an NS-GEV model. Even though the NS-GEV theoretically can model an S-GEV data with a low slope parameter, the increase in variance in adding the fourth parameter contributes to a large nRMSE. For a record length of 50 years, the tradeoff between bias and variance and the question of which misapplication is better depends on other factors such as CV, skewness, time, and amount of nonstationarity. We define a nonstationary index (NSI) as being the estimated change of the mean of the data over a century. At low NSI, the skewness of the data is important with high skewness leading to larger errors in applying the S-GEV. At large NSI, data with low CV or if the project has a long lifespan, the application of the NS-GEV is preferred. If there is ample record length, such as 100 years, the application of NS-GEV is usually preferred since variance is fairly low over such a record length.

Figure 1: the ratio of how much larger the nRMSE is in misapplying the NS-GEV versus correctly applying the S-GEV distribution for the 10-year storm (top) and 100-year storm (bottom).

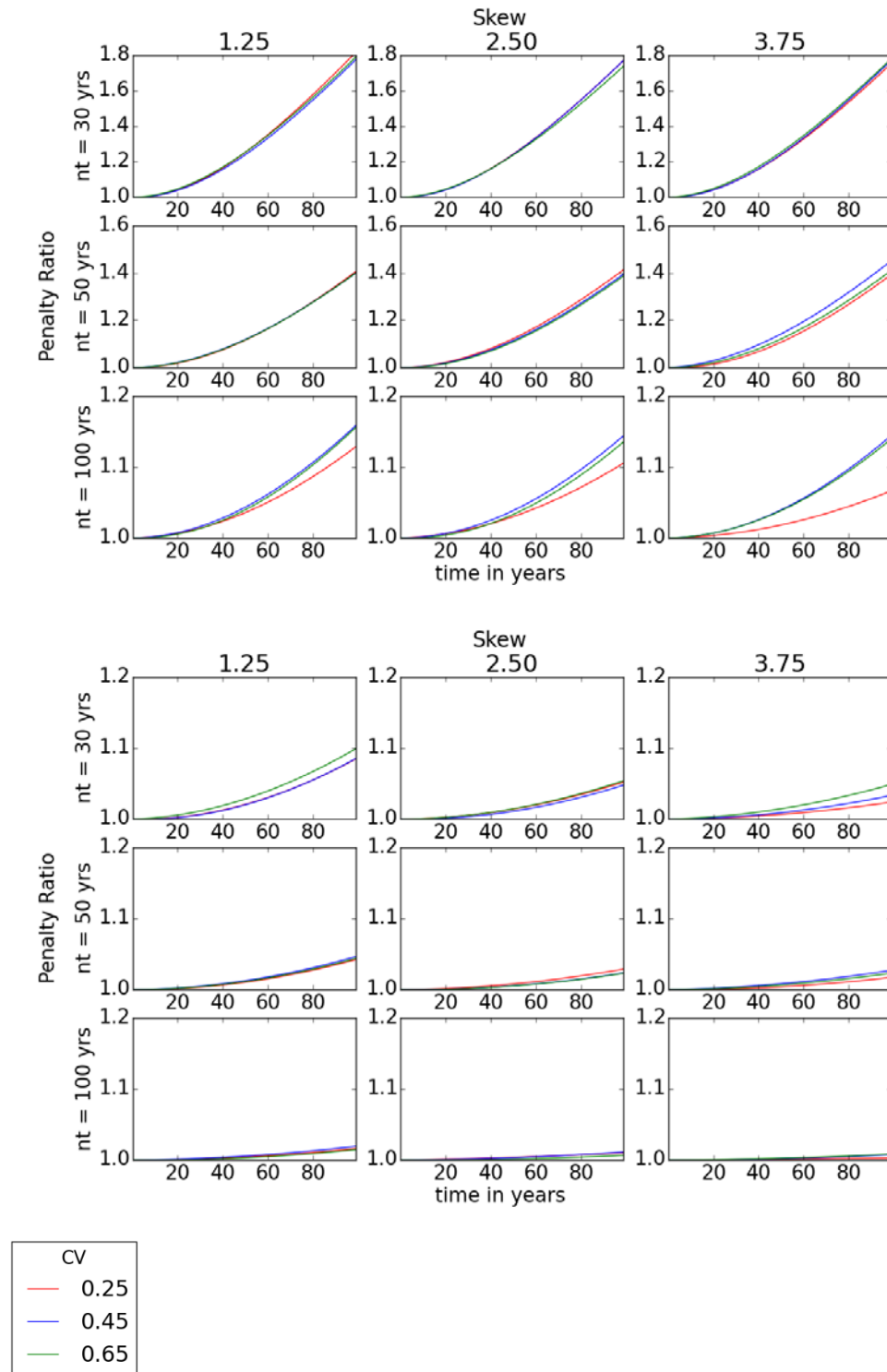


Figure 2: the absolute values of nRMSE from applying an NS-GEV model to an S-GEV environment for the 10-year storm (top) and 100-year storm (bottom) as a function of record length

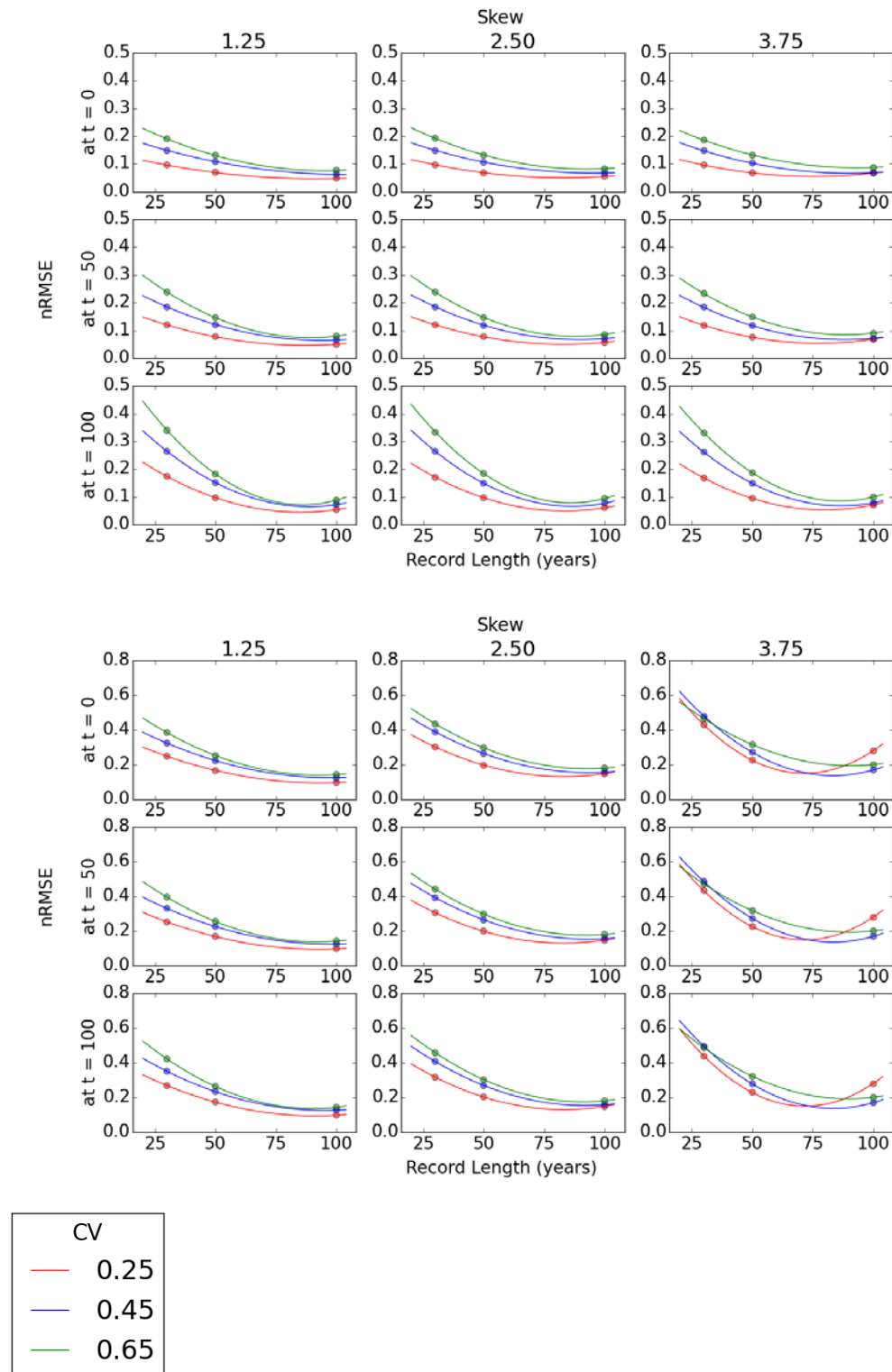
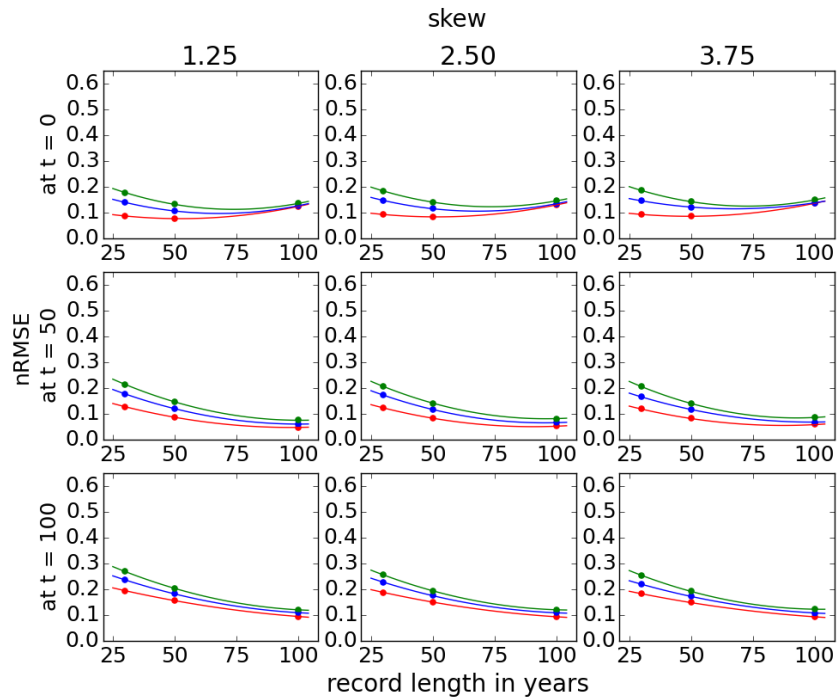
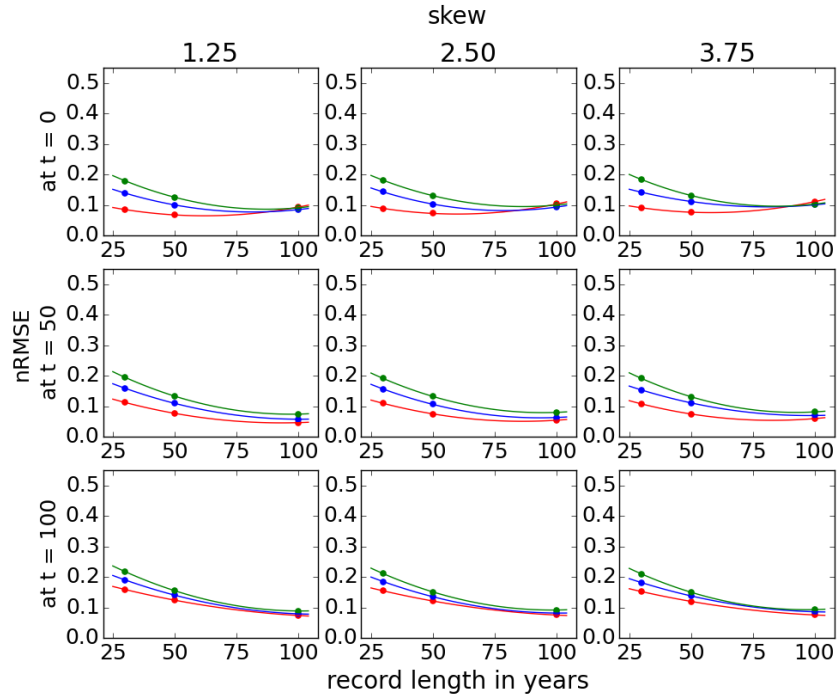
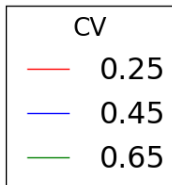
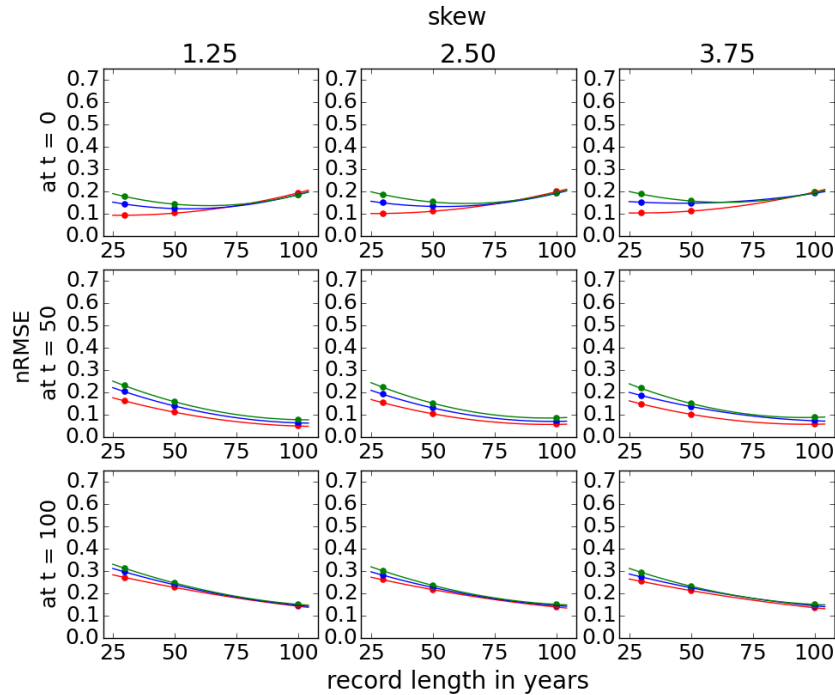


Figure 3: absolute values of nRMSE for the 10-year storm as a function of record length under the three nonstationary scenarios with NSI = 0.1. Scenario I (top), II (middle) and III (bottom) are all shown under these described conditions.





The use of the NS-GEV can be directly translated into creating NS-IDF curves. For IDAF curves, the approach is less studied. We have published a summary of the current state of research in “Best Practices for Incorporating Non-Stationarity in Precipitation-Frequency Estimates”, Chapter 4.2. In moving from station or point data to areal or regionalization, a common flood frequency approach is to use regionalization which involves identifying areas with the same distribution that may be altered by a certain scale, the flood index, but it otherwise identical. We pointed out the need for further research into how potential non-stationarity can be identified within homogeneous regions, how to identify and quantify regional trends, and then to address non-stationarity in regional growth curves as well as areal reduction factors. Some of the characteristics used to determine homogeneity are potentially nonstationary - such as characteristics of rainfall like mean annual precipitation and timing of the wet season. In creating homogeneous regions, it may be of interest to do a sensitivity analysis of the characteristics to changes in time to determine the possible range of error. Another method would be to better include mechanistic drivers of extreme precipitation into the clustering process of regionalization. Currently, statistics represent behavior of the extreme rainfall and are a stand in for these mechanistic drivers. In considering mechanistic drivers of extreme precipitation, stations with the same source of atmospheric moisture or causative circulation pattern are likely to experience similar changes with time. Nonstationarity should be included in regional growth curves and areal reduction factors. Inclusion of a nonstationary distribution into the regional growth curve could be developed similar to the work that has been done for station distributions

previously discussed. It is much more difficult to quantify change in areal reduction factors, however. A stationary assumption could be justified in a carefully homogenized region where the mechanistic drivers of extreme precipitation are the same. Otherwise, it is recommended that in creating nonstationary ARFs, one could include changes in time by comparing the ratio of areal rainfall to point rainfall at various windows of time.

Chapter 2 - MET STATS

Chapter 3 – Atmospheric River Events

Atmospheric rivers are long narrow corridors of high-water vapor content in the atmosphere that originate from tropical or extratropical cyclones. The large influx of water vapor in the region of landfall can result in heavy precipitation and flooding, particularly in orographic regions. ARs have been of particular interest to water resource studies in the Pacific Northwest and northern California; it is now widely accepted that landfalling ARs are related to major flooding events across the coastal western US. To find ARs, we defined an AR as having an integrated water vapor transport (IVT) intensity of either more than 100 kg/m/s or at the 85 percentile and checked our findings against existing AR catalogues to find good agreement. For the AR landfalling dates, we then retrieve precipitation and other hydrometeorological variables (SWE, surface temperature) through our WRF-downscaling of the NCEP-NCAR reanalysis, which serves as both initial conditions and boundary conditions for our modeling.

We chose WRF parameterization schemes and physics processes that were able to replicate believable precipitation events over the PNW and California. We found that the WRF output creates a more consistent field of precipitation and temperature measurements than those found from observational data, which suffer from gauge density particularly in mountainous regions. We then use our temperature and precipitation grids as input for the VIC hydrologic model, which gives us resulting variables of interest such as SWE. We focused on three subregions along the coastal western US: the north Cascades, south Cascades, and Sierra Nevada ranges. Further, we define the cold season as being November to March - the time period in which the bulk of SWE is accumulated. We found that more landfalling ARs occur in the northern subregions, the Cascades, but in general AR events vary temporally as well as spatially, i.e. at different landfalling latitudes. We also considered the effect ARs have on snowpack, as some events will increase SWE while other decrease SWE and found that the timing and the elevation must be considered. Most positive SWE changes occur in January at an elevation band of 2000 - 2500 meters for the Sierra Nevada and at lower elevations of 1000 to 2000 meters for the Cascades. In Figure 4, we show the relationship between the month in which a landfalling AR occurred and the latitude at which it fell. The spatial patterns across the three regions and different elevation bands are shown in Figure 5, and the relationship between duration and AR event is shown in Figure 6. The Sierra Nevada region saw on average nearly twice the increase in January than the Cascades.

Figure 4: reproduced from Eldardiry et al., 2019. Fraction of AR dates from all dates producing the upper 10th percentile of daily precipitation for each latitudinal band by cold season month

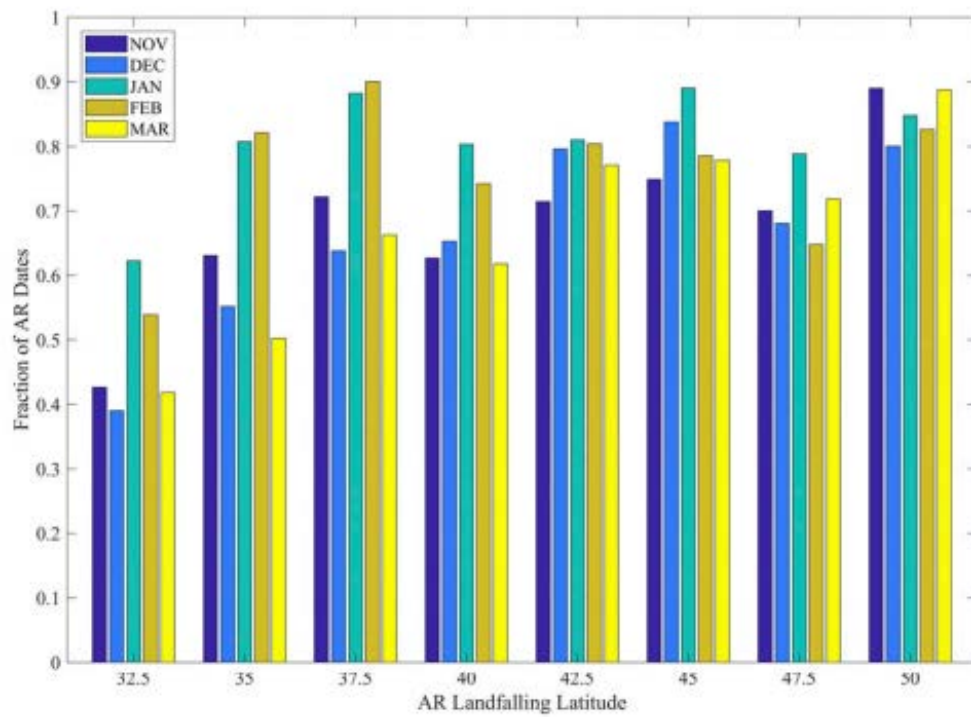


Figure 5: reproduced from Eldardiry et al., 2019. Average of upper 10th percentile positive and negative changes in daily SWE during the upper 10th percentile of daily precipitation on AR dates by winter month.

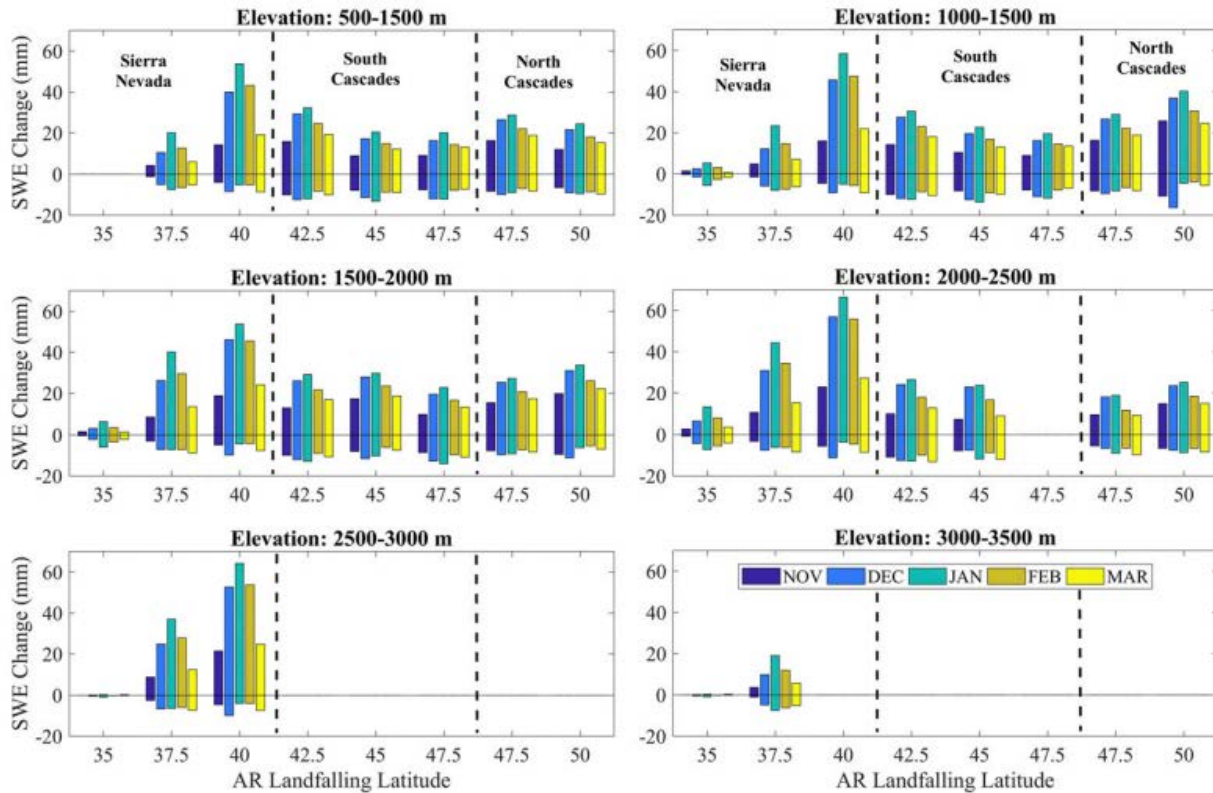
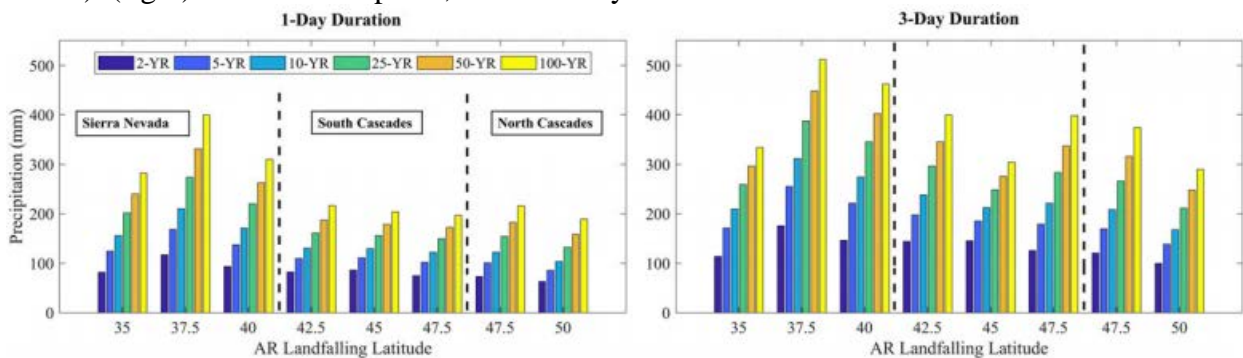
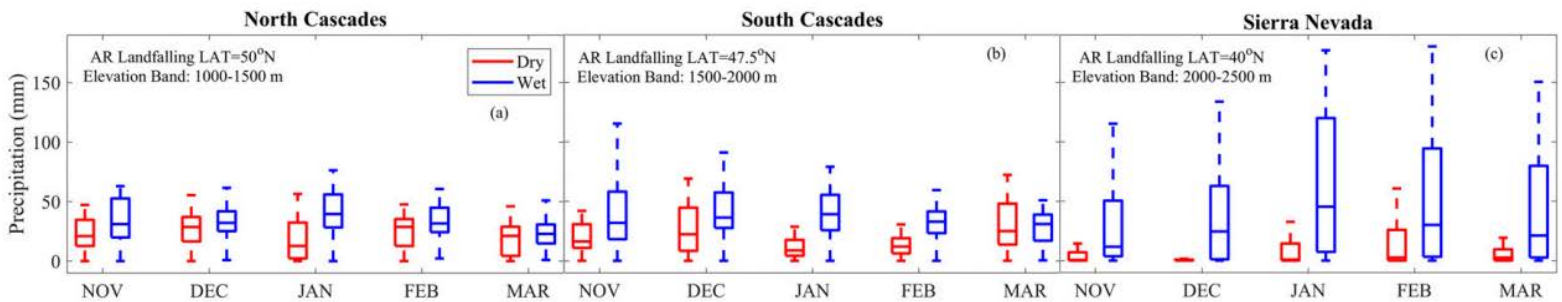


Figure 6: reproduced from Eldardiry et al., 2019. (left) The 1-day AR precipitation depths and frequencies by AR landfalling latitude (return periods are indicated by different colors). (right) As in the left panel, but for 3-day totals.



We found that landfalling ARS within the Sierra Nevada subregion resulted in higher precipitation than the other subregions despite the fact that there were fewer landfalling ARs. Of the landfalling ARs, those having the highest impact on extreme precipitation events happened in January and February. Similarly, the largest increases in SWE associated with ARs also occurs in January, with again, the Sierra Nevada being the most affected. We found that decreases in SWE associated with ARs also occur in the cold months and that high AR-related snowmelt can explain early snowmelt, major flooding events, and increase in rain-on-snow conditions. These results are shown in Figure 7.

Figure 7: reproduced from Eldardiry et al., 2019. Daily precipitation associated with AR dates during dry and wet years in three mountainous subregions (North Cascades, South Cascades, and Sierra Nevada). On each box, the central mark indicates the median depth, and the bottom and top edges of the box indicate the 25th and 75th percentiles (or interquartile range), respectively.



In comparing wet versus dry years, we found that wet years are more numerous than dry years and produce heavier precipitation as well as increases in SWE for the Sierra Nevada region. For the Cascades, the conditions of wet versus dry produce more similar results, although the number of ARs is lower during dry years. Further, for the Cascades region, we found that most AR extreme precipitation events are correlated with warm AR dates. These warm events saw not only extreme precipitation events but also were the catalyst for higher snowmelt rates.

Chapter 4 – Rain-on-snow events

Rain-on-snow events are events where liquid precipitation falls on a pre-existing snowpack and are related to extreme precipitation events and increased runoff and flooding events by decreasing the temperature of the snowpack and priming it for earlier melt onset. ROS can also trigger avalanches if the structural strength of the snowpack is sufficiently reduced. Studies up to now had snowmelt and rainfall contribute to ROS runoff without being able to quantify the contributions of one or the other separately; they also tend to be event based and area specific. We use NCEP-NCAR data, downscaled by WRF, and the VIC model to examine and give an estimate as to the role of ROS on extreme flood events. Specifically, we aimed to find how much ROS contribute to flood runoff versus other snow processes and other energy changes. We addressed spatial patterns over the CONUS but particularly in the western mountain ranges. Further, we considered how ROS contribution to runoff may change under warming climates which we simulate by adding a uniform 2-degree Celsius temperature increase. We use this delta-warming scenario, where other forcing variables remain the same, instead of using

downscaled projections from climate models because we found the changes in precipitation especially as well as some temporal and spatial patterns of in temperature changes were highly variable between models.

We applied the VIC hydrological model to quantify various aspects of the snow mass and energy balance processes which includes transfers via the atmosphere, snow accumulation on overlying vegetation, underlying snowpack conditions, sublimation from the vegetation canopy as well as the underpack, and vegetation related interception. The VIC model parameterization is the same as what is used in a previous study (Livneh et al. 2015). We created hourly simulations for the time period of 1950 to 2013 and found these parameters simulate snow and streamflow well as compared to observations. For observations, we used a network of 300 streamflow gauges which had a long record length of 50 years. We also compared our simulations to the Sierra Nevada SWE analysis data set (Margulis et al., 2016) which is a high-resolution gridded dataset which take into account Landsat observations. Then we compared 100-year flood magnitude estimates from the three different sets of data (our simulated data, the observation data, and the SNSR data) as well as the cumulative distribution function of the AMS extracted from streamflow data and found good agreement between datasets.

We examine the ratio between the number of large ROS days and large runoff days across the CONUS. The areas most susceptible to feeling effects of ROS include the mountain ranges along the Western, Upper Midwest, Northwest CONUS and the Appalachian ranges. The PNW is the most impacted by ROS with the greatest frequency of ROS events due to the area's relationship with orographic rainfall and deep snowbanks. This spatial pattern is shown in Figure 8. Through the setup and use of the VIC hydrological model, we are also able to find the fractional contribution to ROS runoff from rainfall and from snowmelt separately. We found that snowmelt largely dominates large ROS events in the Rockies, Northeast, and Upper Midwest - regions with fairly mild rainfall magnitude and frequency and have a later water year than what constitutes of the water year in the West coast. On the other hand, along the West Coast, we found that rainfall accounts for up to 70% of the large ROS events due to being coastal areas impacted by ARs, which magnify orographic rainfall and lead to intense rainfall events. These results are shown in Figure 9.

Figure 8: reproduced from Li et al., 2019. Fractional contribution of the number of large and extreme ROS days to the number of (a) total large runoff days, (b) total extreme runoff days, (c) total large runoff, (d) total extreme runoff. The white areas in the maps have mean annual maximum snow water equivalent less than 20 mm and are excluded in the analysis.

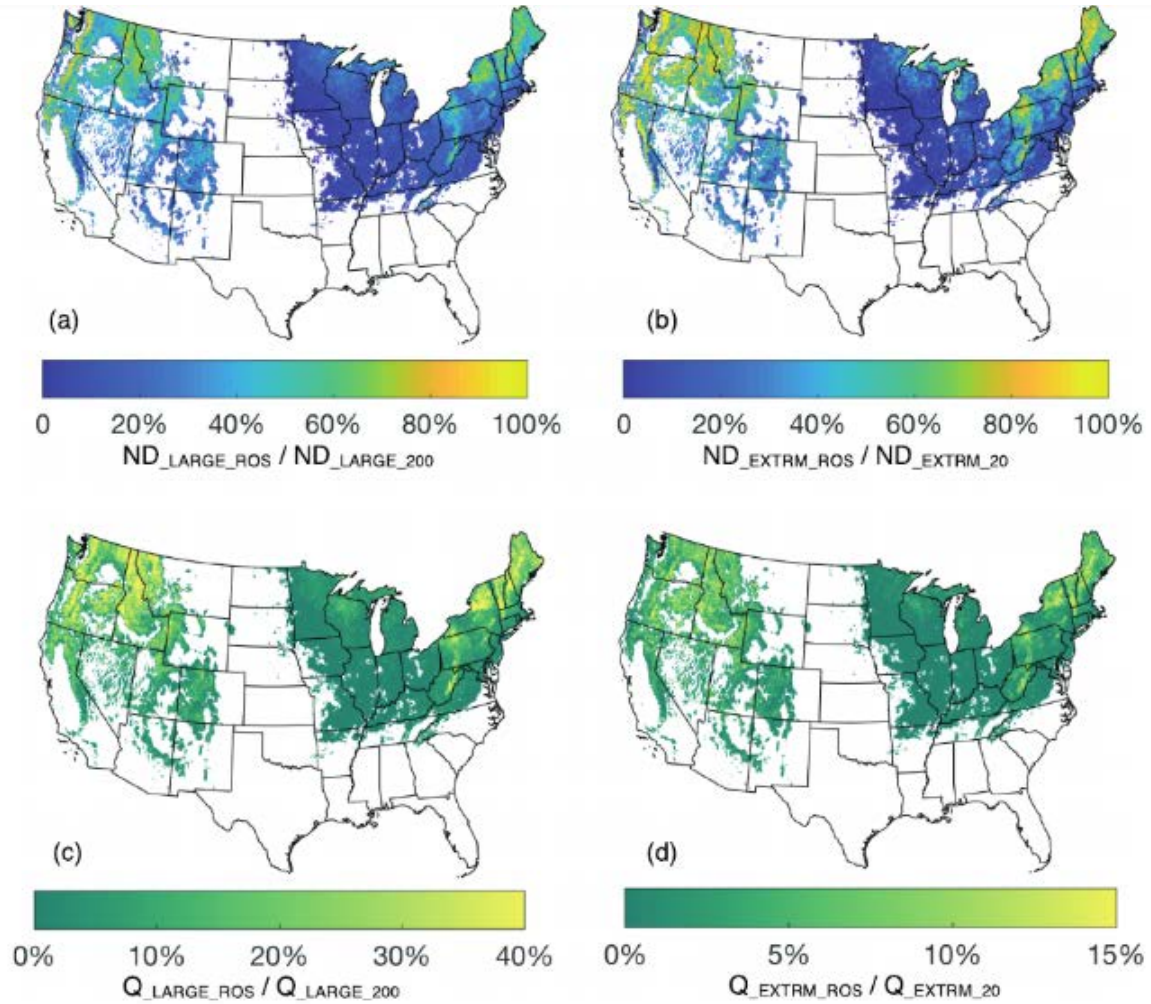
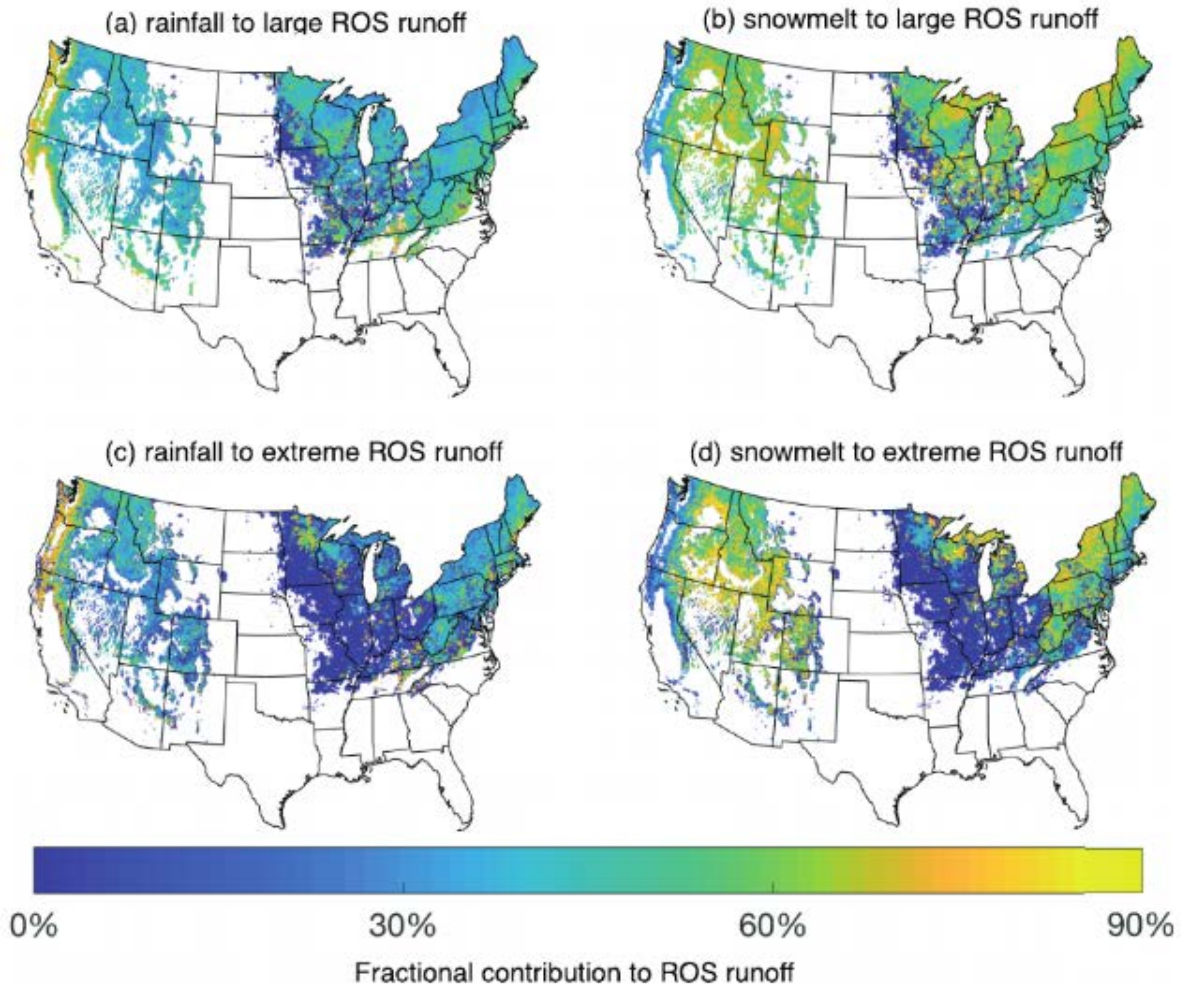
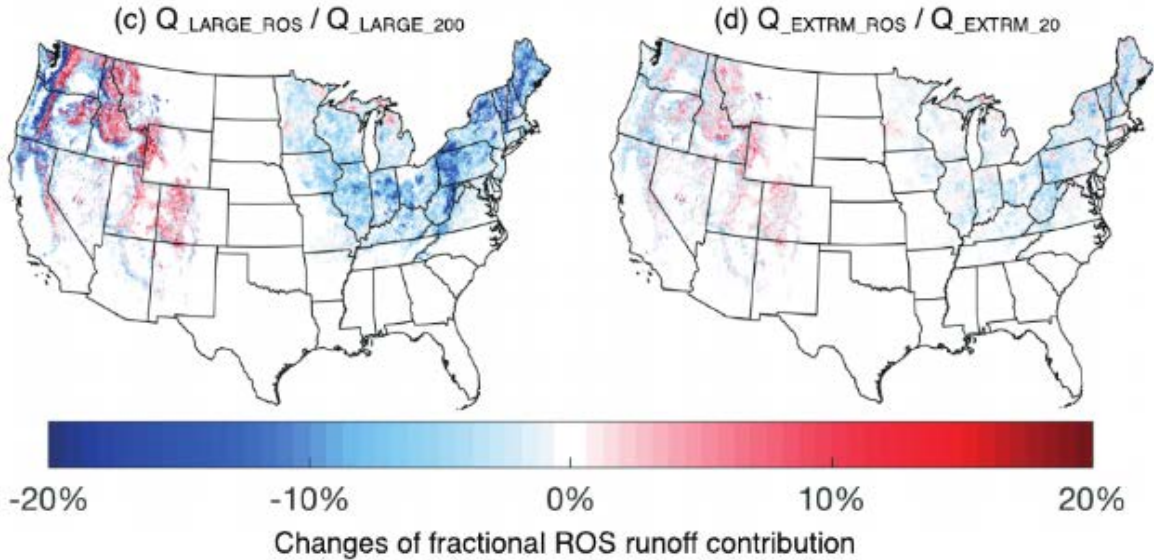


Figure 9: reproduced from Li et al., 2019. Fractional contribution to the large and extreme ROS runoff from rainfall and snowmelt. (a) and (b) show the ratio of the rainfall and snowmelt from the large ROS days (i.e., the ROS days in the 200 large runoff days) to the total large ROS runoff (i.e., the total runoff from the large ROS days), respectively. (c) and (d) show the ratio of the rainfall and snowmelt from the extreme ROS days (i.e., the ROS days in the 20 extreme runoff days) to the total extreme ROS runoff (i.e., the total runoff from the extreme ROS days), respectively. White areas in the maps have mean annual maximum snow water equivalent less than 20mm and are excluded from the analysis.



In a warmer future, we found through simulations that ROS events will increase at high-elevation bands of the mountains (>2000 m) and will decrease if lower than that band. As a result of their elevation profiles, ROS events will have less impact over the Midwest and much of the eastern US. However, the change of ROS frequency will be critical in managing water resources along the West coast; when using the same precipitation forcings, future changes of runoff contributions from ROS to extreme floods will be paramount. Our model results cannot be used for planning or prediction purposes but show that the impact of ROS in the West coast is sensitive to changes in temperature. Changes in fractional ROS runoff contributions in this warm scenario are shown in Figure 10.

Figure 10: reproduced from Li et al., 2019. Change in the ratio of total runoff during large ROS days (left) and extreme ROS days (right) to total runoff from the 200 large (or extreme) runoff days. White areas have historical mean annual maximum snow water equivalent less than 20 mm and are excluded in the analysis



Conclusions and Implications for Future Research/Implementation

In our work, we examined how different facets of global warming would affect three different hydrological processes and how these changes could lead to changes in future flood risk. For extreme precipitation events, we discussed the 10-year and 100-year design storms in the context of extreme value theory. We introduced a time-varying parameter into the mean of the data and ran Monte Carlo simulations to find the misapplication of either the S-GEV or NS-GEV distribution with regards to the environment will vary depending on the data CV, skewness, record length, and time. The application of the S-GEV is associated with lower variance but increasing bias with time, resulting in increasing error in time. The application of the NS-GEV is associated with increased variance due to the inclusion of a fourth parameter, but possibly lower bias with time as the NS-GEV is more capable of adjusting to model a S-GEV environment than vice versa (the S-GEV model cannot adapt for a NS-GEV environment). We found that for short record lengths of thirty years, while the NS-GEV can sometimes recreate near-stationary conditions, the increase in variance offsets any possible decreases in bias. When the record length is at fifty years, we find the tradeoff between variance and bias is more closely matched. The particulars of which misapplication is “better” – i.e. results in lower nRMSE – depends on the data characteristics such as CV, skewness, and amount of nonstationarity present in the NS-GEV environment, and time. For very low amounts of nonstationarity present, the S-GEV is still preferred for short-term usage. However, as the time (i.e. lifespan) increases or as the amount of nonstationarity (NSI) increases, the NS-GEV is more favorable. If the record length is exceptionally long, such as 100 years, the application of the S-GEV is only preferred for the very early years of a project’s lifespan. As time increases, the nRMSE associated with the

misapplication of the S-GEV is larger than that of the NS-GEV. Ultimately, deciding which model of the GEV distribution to apply to an AMS with an unknown stationary assumption, should take into particular consideration the record length available as well as the project lifespan required. To a smaller degree, the decision will be based on the data CV and skewness.

Establishing a nonstationary distribution function has direct implications for the construction of IDF and IDAF curves which civil engineers use to understand flood risk. Accurate flood risk assessment will include a time-varying parameter to reflect the changing climate we are experiencing now. Without this updated methodology, projects risk being inappropriately sized and lead to either increased expenses due to highly damaging floods or increased expenses in over-sizing a project, which has its own costs. Our work indicates that future work would benefit from looking at whether CV changes with time and how. The change in CV with time will affect the resulting error of design storms. More research is needed to better understand how to accurately reflect a nonstationary scale parameter (in addition to a nonstationary location parameter) which currently requires an incredibly long station record for meaningful results. Work could also be done to find more accurate measures of nonstationarity that lead to lower variance increases in the error. This is particularly important for stations with short record lengths. Further research could also be conducted as to how to include nonstationarity into the other mentioned distributions, such as Lognormal, logistic, Pearson III, and Gumbel.

ARs play an important role in the water cycle over the western US by influencing key hydrological processes such as SWE accumulation, snowmelt rates, and timing of peak SWE. Further, they are particularly important as drought busters. We found that landfalling ARs have different influences on precipitation depending on the location (latitude) and elevation at which they land. Landfalling ARs in the Sierra Nevada subregion of our study resulted in higher precipitation amounts despite fewer events than in the Cascade subregions. For all study areas, the most extreme events occur in January and February. Further, January sees the highest increase in SWE as related to AR events across all subregions. The Sierra Nevada sees higher snow accumulations than the Cascades. However, SWE decreases are also known to happen with AR events in other cold months and the resulting snowmelt can explain early snowmelt and increased chances of ROS conditions. In the Sierra Nevada, ARs during wet years are more frequent than dry years and also produce heavier precipitation and snow accumulation per event. For the Cascades, however, the amount of precipitation and snow accumulation are fairly equal. The number of AR events is more frequent in wet years than dry years for these subregions as well. Most AR extreme precipitation events in norther latitudes occur during warm AR dates and result in lower SWE accumulation, or higher snowmelt rates, which can significantly impact snowpack structure and strength. The Cascades are more susceptible to increased snowmelt rates with AR events than the Sierra Nevada.

A better understanding of ARs is essential to efficient water management in the western US. ARs affect flood events via increased snowmelt rates and can end drought conditions. Further work should be done first and foremost in increasing our ability to detect and forecast ARs. Research on ARs is fairly recent and our understanding of historical ARs is limited due to the dependency of AR characterization on variables that were difficult to measure in the past. The second main body of work needed for understanding the effects of landfalling ARs is in being able to characterize ARs by different aspects such as elevation, latitude, conditions such as being a warm year or a dry year. Our work found that these characteristics have noticeably different resulting impacts on precipitation and SWE. Other characteristics could be investigated

such as aspect and slope of the topography as related to the physical properties of the AR. Understanding spatial differences in AR characteristics will be key in developing better forecasting methods. More research should also be done on how the effects of ARs will change with global warming – snow melting rates are likely to increase; the timing of peak SWE is likely to shift to being earlier; and the snow-melt related runoff will be impacted as a result of these changes. Since snowmelt runoff is a key component of the water budget in the west, future work should be done for a more detailed understanding of the impacts of AR precipitation and runoff with global warming.

We characterized historical and future ROS conditions across the CONUS and found that the main regions impacted by ROS events are the major western mountain ranges, parts of the Upper Midwest and Northeast, as well as the lower Appalachian region. The contribution of ROS to extreme runoff in the western US has been at mid-elevation areas that we title the “significant influence zone”. In conducting a kind of sensitivity analysis, we found that this elevation band is likely to shift higher in the future with global warming, and the importance of ROS events will decrease in the eastern US and Midwest but will increase in importance along the western US. Presently, ROS occur mostly in the fall and winter along the coastal West and eastern US while they occur mostly in spring for the high mountains in the west. From our work, we also found that while a significant portion of large and extreme runoff events are related to ROS events, total runoff from ROS days account for only a modest part of the overall runoff. This indicates that most extreme rainfall is rather the result of intense rainfall or radiation-driven snowmelt even when ROS conditions are active. Net radiation dominates snowmelt on ROS days in the west while net radiation and turbulent heat flux dominates in the eastern US.

There is further work to be done on modeling how ROS will respond to global warming as predicted by GCMs and RCMs rather than from our sensitivity analysis to increases in temperature. Our delta warming method is simplified in some respects such as not considering any changes in precipitation with temperature changes. It is likely, however, that precipitation patterns, frequency, and intensity will change with global warming and the new inputs of precipitation for modeling the effects of ROS will be critical to a more accurate understanding of how ROS effects will change with time. Also, the change in timing of the ROS shifting to be earlier impacts characteristics of the snowpack. Further work should be done in understanding exactly how much these changes can impact snowpack accumulation and structural strength in particular, as these are key to predicting snowmelt related flooding events.

Literature Cited

- Andreadis, K., P. Storck, and D. P. Lettenmaier, 2009: Modeling snow accumulation and ablation processes in forested environments. *Water Resources Research*, 45.
- Armstrong, A., S. Waldron, J. Whitaker, N.J. Ostle, 2014: Wind farm and solar park effects on plant-soil carbon cycling: uncertain impacts of changes in ground-level microclimate. *Global Change Biology*, 20(6).
- Barth, N. A., G. Villarini, M. A. Nayak, and K. White, 2017: Mixed populations and annual flood frequency estimates in the western United States: The role of atmospheric rivers. *Water Resource Research*, 53, 257–269.
- Bergman, J. A., 1987: Rain-on-snow and soil mass failure in the Sierra Nevada of California. *Landslide Activity in the Sierra Nevada during 1982 and 1983*, 15– 26. San Francisco, CA, USA: USDA Forest Service.
- Cheng, L., AghaKouchak, A., Gilleland, E., & Katz, R. W., 2014: Non-stationary extreme value analysis in a changing climate. *Climatic Change*, 127(2), 353– 369.
- Conway, H., Breyfogle, S., Wilbour, C.R., 1988: Observations relating to wet snow stability. *International Snow Science Workshop, ISSW'88 Commission*, Whistler, B.C., Canada.
- Conway, H., & Raymond, C. F., 1993: Snow stability during rain. *Journal of Glaciology*, 39(133), 635– 642.
- Daly, C., Taylor, G. H., & Gibson, W. P., 1997: The PRISM approach to mapping precipitation and temperature. In *Proc., 10th AMS Conf. on Applied Climatology*, 20-23.
- Dettinger, M., 2011: Climate change, atmospheric rivers, and floods in California—A multimodel analysis of storm frequency and magnitude changes. *Journal American Water Resource Association*, 47, 514–523.
- Dettinger, M., 2013: Atmospheric rivers as drought busters on the U.S. West Coast. *Journal of Hydrometeorology*, 14, 1721–1732.
- Dettinger, M., F. M. Ralph, T. Das, P. J. Neiman, and D. R. Cayan, 2011: Atmospheric rivers, floods and the water resources of California. *Water*, 3, 445–478.
- Dettinger, M., F. M. Ralph, and J. J. Rutz, 2018: Empirical return periods of the most intense vapor transports during historical atmospheric river landfalls on the U.S. West Coast. *Journal of Hydrometeorology*, 19, 1363–1377.
- Easterling, David R., G. A. Meehl, C. Parmesan, S. A. Changnon, T. R. Karl, and L. O. Mearns, 200: Climate extremes: observations, modeling, and impacts. *Science*, 289(5487), 2068-2074.

- Easterling, D.R., K.E. Kunkel, J.R. Arnold, T. Knutson, A.N. LeGrande, L.R. Leung, R.S. Vose, D.E. Waliser, and M.F. Wehner, 2017: Precipitation change in the United States. Climate Science Special Report: Fourth National Climate Assessment, Volume I, 207-230.
- Falcone, J. A., Carlisle, D. M., Wolock, D. M., & Meador, M. R., 2010: GAGES: A stream gage database for evaluating natural and altered flow conditions in the conterminous United States. *Ecology*, 91(2), 621– 621.
- Frich, P., L. V. Alexander, P. Della-Marta, B. Gleason, M. Haylock, A. M. G. Klein Tank, and T. Peterson, 2002: Observed coherent changes in climatic extremes during the second half of the twentieth century. *Climate Research*, 19(3), 193-212.
- Groisman, P.Y., R.W. Knight, and O.G. Zolina, 2014: Recent trends in regional and global intense precipitation patterns, Section 5.03 in *Climate Vulnerability*. Water Resources Volume, F. Hossain, ed., 25-56.
- Guan, B., Waliser, D. E., Ralph, F. M., Fetzer, E. J., & Neiman, P. J. 2016: Hydrometeorological characteristics of rain-on-snow events associated with atmospheric rivers. *Geophysical research letters*, 43, 2964– 2973.
- Hamlet, A.F., and D.P. Lettenmaier, 2007: Effects of 20th century warming and climate variability on flood risk in the western U.S. *Water Resources Research*, 43.
- Harr, R. D., 1981: Some characteristics and consequences of snowmelt during rainfall in western Oregon. *Journal of Hydrology*, 53(3-4), 277– 304.
- Heywood, L., 1988: Rain on snow avalanche events—Some observations. *Proceedings of the International Snow Science Workshop. ISSW'88 Comm., Whistler, B.C., Canada.*
- Hirsch, R.M., and K.R. Ryberg, 2012: Has the magnitude of floods across the USA changed with global CO2 levels?. *Hydrological Sciences Journal*, 57.
- Hong, S. Y., Y. Noh, and J. Dudhia, 2006: A new vertical diffusion package with an explicit treatment of entrainment processes. *Monthly Weather Review*, 134, 2318–2341.
- Hosking J.R.M., and J.R. Wallis, 1997. *Regional Frequency Analysis - An Approach Based on L-Moments*, Cambridge Press.
- Hungerford, R. D., Nemani, R. R., Running, S. W., & Coughlan, J. C., 1989: MTCLIM: A mountain microclimate simulation model. Res. Pap. INT-RP-414. Ogden, UT: US Department of Agriculture, Forest Service, Intermountain Research Station, 52.
- Jordan, R., 1991: A one-dimensional temperature model for a snow cover: Technical documentation for SNTERRM.89. Special Rep. 91–16, Cold Region Research and Engineers Laboratory, U.S. Army Corps of Engineers, Hanover, NH.
- Kain, J., 2004: The Kain–Fritsch convective parameterization: An update. *Journal Applied Meteorology*, 43, 170–181.
- Kain, J., and J. Fritsch, 1990: A one-dimensional entraining/detraining plume model and its application in convective parameterization. *Journal Atmospheric Sciences*, 47, 2784–2802.

Kain, J., and J. Fritsch, 1993: Convective parameterization for mesoscale models: The Kain–Fritsch scheme. *The Representation of Cumulus Convection in Numerical Models*. Meteor. Monogr., No. 46, American Meteorological Society, 165–170.

Karl, Thomas R. and R. W. Knight, 1998: Secular trends of precipitation amount, frequency, and intensity in the United States. *Bulletin of the American Meteorological Society*, 79, 231-241.

Kendall, M. G. 1975: *Rank correlation methods*, (4th ed.). London: Charles Griffin.

Konrad, C. P., and M. D. Dettinger, 2017: Flood runoff in relation to water vapor transport by atmospheric rivers over the Western United States, 1949–2015. *Geophysical Research Letters*, 44, 11,456–11,462.

Kunkel, K.E., K. Andsager, and D.R. Easterling, 1999: Long-term trends in extreme precipitation events over the conterminous United States and Canada. *Journal of Climate* 12, 2515–2527.

Kunkel, K.E., et al., 2013: Monitoring and understanding trends in extreme storms: State of knowledge. *Bulletin American Meteorological Society*, 94, 499-514.

Lamjiri, M. A., M. D. Dettinger, F. M. Ralph, and B. Guan, 2017: Hourly storm characteristics along the US West Coast: Role of atmospheric rivers in extreme precipitation. *Geophysical Research Letters*, 44, 7020–7028.

Liang, X., D.P. Lettenmaier, E. F. Wood and S.J. Burges, 1994: A simple hydrologically based model of land surface model of land surface water and energy fluxes for general circulation models. *Journal Geophysical Research*, 99, 14,415-14,428.

Liang, X., D. P. Lettenmaier, and E. F. Wood, 1996: One-dimensional statistical dynamic representation of subgrid spatial variability of precipitation in the two-layer variable infiltration capacity model. *Journal Geophysical Research*, 101, 21,403-21,422.

Liang, X., E.F. Wood, and D.P. Lettenmaier, 1996: Surface soil moisture parameterization of the VIC- 2L model: Evaluation and modifications. *Global and Planetary Change*, 13, 195-206.

Liang, X., E.F. Wood, and D.P. Lettenmaier, 1999: Modeling ground heat flux in land surface parameterization schemes. *Journal Geophysical Research*, 104, 9,581-9,600.

Lins, H.F., and J.R. Slack, 1999: Streamflow trends in the United States. *Geophysical Research Letters*, 26, 227-230.

Lins, H.F., and J.R. Slack, 2005: Seasonal and regional characteristics of U.S. streamflow trends from 1940 to 1999. *Physical Geography*, 26, 489-501.

Livneh, B., E.A. Rosenberg, C. Lin, B. Nijssen, V. Mishra, K. Andreadis, E.P. Maurer, and D.P. Lettenmaier, 2013: A long-term hydrologically based data set of land surface fluxes and states for the conterminous United States: Updates and extensions. *Journal of Climate*.

Livneh, B., Bohn, T. J., Pierce, D. W., Munoz-Arriola, F., Nijssen, B., Vose, R., Cayan, D. R., & Brekke, L., 2015: A spatially comprehensive, hydrometeorological data set for Mexico, the US, and Southern Canada 1950–2013. *Scientific Data*, 2(1).

Margulis, S. A., Cortés, G., Giroto, M., & Durand, M., 2016: A Landsat-era Sierra Nevada snow reanalysis (1985–2015). *Journal of Hydrometeorology*, 17(4), 1203– 1221.

McMahon, G., S. M. Gregonis, S. W. Waltman, J. M. Omernik, T. D. Thorson, J. A. Freeouf, A. H. Rorick, and J. E. Keys, 2001: Developing a spatial framework of common ecological regions for the conterminous United States. *Environmental Management*, 28, 293–316.

Min, Seung-Ki, X. Zhang, F. W. Zwiers, and G. C. Hegerl, 2010: Human contribution to more-intense precipitation extremes. *Nature*, 470, 378-381.

Mishra, V., and D.P. Lettenmaier, 2011: Climatic trends in major U.S. urban areas, 1950-2009. *Geophysical Research Letters*, 38.

Mishra, V., F. Dominguez, and D.P. Lettenmaier, 2012: Urban precipitation extremes: how reliable are regional climate models?. *Geophysical Research Letters*, 39, L03907.

Morrison, H., G. Thompson, and V. Tatarskii, 2009: Impact of cloud microphysics on the development of trailing stratiform precipitation in a simulated squall line: Comparison of one- and two-moment schemes. *Monthly Weather Review*, 137, 991–1007.

Neiman, P. J., F. M. Ralph, G. A. Wick, J. D. Lundquist, and M. D. Dettinger, 2008: Meteorological characteristics and overland precipitation impacts of atmospheric rivers affecting the West Coast of North America based on eight years of SSM/I satellite observations. *Journal of Hydrometeorology*, 9, 22–47.

Neiman, P. J., A. B. White, F. M. Ralph, D. J. Gottas, and S. I. Gutman, 2009: A water vapour flux tool for precipitation forecasting. *Proc. Institute Civil Engineering: Water Management*, 162, 83–94.

Neiman, P. J., Schick, L. J., Ralph, F. M., Hughes, M., & Wick, G. A., 2011: Flooding in western Washington: The connection to atmospheric rivers. *Journal of Hydrometeorology*, 12(6), 1337– 1358.

Omernik, J. M., 2004: Perspectives on the nature and definition of ecological regions. *Environmental Management*, 34, S27–S38.

Ralph, F. M., & Dettinger, M. D., 2011: Storms, floods, and the science of atmospheric rivers. *EOS, Transactions American Geophysical Union*, 92(32), 265– 266.

Ralph, F. M., Neiman, P. J., Kingsmill, D. E., Persson, P. O. G., White, A. B., Strem, E. T., Andrews, E. D., & Antweiler, R. C., 2003: The impact of a prominent rain shadow on

flooding in California's Santa Cruz Mountains: A CALJET case study and sensitivity to the ENSO cycle. *Journal of Hydrometeorology*, 4(6), 1243– 1264.

Ralph, F. M., and M. D. Dettinger, 2012: Historical and national perspectives on extreme West Coast precipitation associated with atmospheric rivers during December 2010. *Bulletin of American Meteorological Society*, 93, 783–790.

Ralph, F. M., P. J. Neiman, G. A. Wick, S. I. Gutman, M. D. Dettinger, D. R. Cayan, and A. B. White, 2006: Flooding on California's Russian River: Role of atmospheric rivers. *Geophysical Research Letters*, 33, L13801.

Ralph, F. M., T. Coleman, P. J. Neiman, R. J. Zamora, and M. D. Dettinger, 2013: Observed impacts of duration and seasonality of atmospheric-river landfalls on soil moisture and runoff in coastal northern California. *Journal of Hydrometeorology*, 14, 443–459.

Ralph, F. M., et al., 2014: A vision for future observations for western U.S. extreme precipitation and flooding. *Journal of Contemporary Water Resource Education*, 153, 16–32.

Singh, P., Spitzbart, G., Hübl, H., & Weinmeister, H. W., 1997: Hydrological response of snowpack under rain-on-snow events: A field study. *Journal of Hydrology*, 202(1-4), 1– 20.

Ter Braak, C.J.F., 2006: A Markov Chain Monte Carlo version of the Genetic Algorithm Differential Evolution: easy Bayesian computing for real parameter spaces. *Statistics and Computing*, 16, 239-249.

Trenberth, Kevin E., 2011: Changes in precipitation with climate change. *Climate Research*, 47(1/2), 123-138.

Vrugt, J. A., Ter Braak, C. J. F., Diks, C. G. H., Robinson, B. A., Hyman, J. M., & Higdon, D., 2009: Accelerating Markov chain Monte Carlo simulation by differential evolution with self-adaptive randomized subspace sampling. *International Journal of Nonlinear Sciences and Numerical Simulation*, 10(3), 273– 290.

Westra, S., L.V. Alexander, and F.W. Zwiers, 2013: Global increasing trends in annual maximum daily precipitation. *Journal of Climate*, 26.

Appendices

Supporting Data

The NCEP–NCAR AR catalog:
<https://ucla.box.com/ARcatalog>.

The WRF downscaled reanalysis data:
<https://www.dropbox.com/home/Public/SERDP/Northwest>.

Livneh meteorological forcings:
<https://data.nodc.noaa.gov/thredds/catalog/nodc/archive/data/0129374/daily/catalog.html>

GAGES II data:
https://water.usgs.gov/GIS/metadata/usgswrd/XML/gagesII_Sept2011.xml#stdorder

SNSR SWE:
<https://margulis-group.github.io/data/>

USGS streamflow observations:
https://waterdata.usgs.gov/nwis/uv/?referred_module=sw

VIC hydrologic model:
<https://github.com/UW-Hydro/VIC/releases/tag/VIC.4.2.d>

NEVA flood risk estimation scheme:
<http://amir.eng.uci.edu/neva.php>

We also uploaded all the data used to reproduce the results in this paper and other useful modeling outputs to a public repository (at <https://doi.org/10.6084/m9.figshare.8244398>).

List of Publications

Eldardiry, H., A. Mahmood, X. Chen, F. Hossain, B. Nijssen and D.P. Lettenmaier, 2019: Atmospheric River-Induced Precipitation and Snowpack during the Western United States Cold Season, *Journal of Hydrometeorology*, DOI:10.1175/JHM-D-18-0228.1.

Li, D., Lettenmaier, D.P., Margulis, S.A., Andreadis, K.M., 2019: The role of rain-on-snow in flooding over the conterminous United States, *Water Resources Research*, DOI:10.1029/2019WR024950.